Phi: Jurnal Pendidikan Fisika dan Terapan
Vol. 12, No. 2 (2026) 316-331
ISSN: 2460-4348, e-ISSN: 2549-7162
https://jurnal.ar-raniry.ac.id/index.php/jurnalphi/index

Article Type: *original research*

Application of the Adam Gradient Descent Optimizer (AGDO) for One-Dimensional Magnetotelluric (MT) Data Inversion

M. Fadhilah Al Yasir Harahap[1], Selvi Misnia Irawati[1], Wahyu Eko Junian[1*]
[1]Department of Geophysical Engineering, Faculty of Industrial Technology, Institut Teknologi Sumatera

Correspondence E-mail: wahyu.junian@tg.itera.ac.id

ARTICLE INFO

Article History:
Received: 11 April 2026
Revised: 24 May 2026
Accepted: 08 July 2026
Published: 19 July 2026

Keywords:
Electromagnetic, Magnetotelluric; Inverse modelling; Resistivity; Adam gradient descent Optimizer

ABSTRACT

This study investigates the application of the Adam Gradient Descent Optimizer (AGDO) for one-dimensional (1D) magnetotelluric (MT) inversion. The algorithm was evaluated using a benchmark function, synthetic MT datasets generated from layered Earth models with 5% Gaussian noise, and field MT data from the Cloncurry region, Australia. For the synthetic datasets, AGDO successfully reconstructed the target resistivity structures, yielding RMSE values ranging from 0.0599 to 0.0603 across four models with different resistivity configurations. For the field datasets, the inversion produced RMSE values between 0.0225 and 0.0582, indicating good agreement between the observed and calculated responses. The ensemble of models obtained from 100 independent runs clustered around the best-fit solutions, demonstrating stable convergence and consistent inversion results despite different random initial populations. These results indicate that AGDO provides an effective and reliable optimization framework for one-dimensional MT inversion and represents a promising alternative for addressing the nonlinear and non-unique nature of the problem.

This work is licensed under a Creative Commons Attribution-ShareAlike 4.0 International License

1. INTRODUCTION

The magnetotelluric (MT) method is a passive electromagnetic geophysical technique that utilizes variations in the Earth's electric and magnetic fields to investigate subsurface electrical conductivity. This approach provides information on resistivity structures from shallow depths to several hundred kilometers, making it widely applicable in geothermal, mineral, and hydrocarbon exploration, as well as in studies of the Earth's crust and mantle structure (Chave & Jones, 2021; Simpson & Bahr, 1997). Variations in the electromagnetic field measured at the Earth's surface are used to calculate the impedance resistivity model.

In MT data interpretation, a one-dimensional (1-D) modeling approach is frequently employed as an initial analytical step. The 1D model assumes the subsurface consists of horizontal layers with constant resistivity (Pedersen & Hermance, 1986). This approach involves fewer parameters than two-dimensional or three-dimensional models, resulting in a more stable inversion process and facilitating early-stage data analysis (Constable et al., 1987). Consequently, 1-D modeling is commonly used to provide an overview of subsurface resistivity characteristics prior to more complex analyses (Oryński et al., 2022).

A primary challenge in MT data interpretation is the inversion process, which involves identifying subsurface models that generate theoretical responses that closely match the observed data. The inversion problem is inherently nonlinear and non-unique, meaning multiple subsurface models can produce similar electromagnetic responses (Parker, 1983). Additionally, model equivalence often arises, in which distinct models yield nearly identical data responses. These characteristics increase the complexity of the inversion process and necessitate optimization approaches that can more effectively explore the solution space (Dell'aversana, 2023; Grandis, 1999; Hu et al., 2025).

Various inversion methods have been developed to address these challenges. Deterministic algorithms, including Occam inversion (Wijaya et al., 2016), Gauss-Newton (Li et al., 2026), and nonlinear conjugate gradient (Rodi & Mackie, 2001), are widely used in MT data processing due to their efficiency in minimizing the error between observed data and model responses (Siripunvaraporn, 2012). However, deterministic algorithms are highly sensitive to the choice of initial model and may become trapped in local minima, particularly when the relationship between model parameters and observed data is highly nonlinear (Liu et al., 2022).

To overcome these limitations, metaheuristic optimization algorithms have increasingly been applied in geophysical inversion. These algorithms perform global searches over the parameter space, thereby increasing the likelihood of identifying near-global solutions and providing better assessments of uncertainty and model stability (Goyes-Peñafiel et al., 2025; Mukesh et al., 2023; Syaripudin & Grandis, 2001). Previous studies have demonstrated the successful application of algorithms such as Particle Swarm Optimization (PSO), Grey Wolf Optimizer (GWO), and One-to-One-Based Optimizer (OOBO) to one-dimensional MT inversion (Grandis & Maulana, 2017; Junian et al., 2023; Junian et al., 2025; Junian et al., 2026).

Although these algorithms have shown promising results, each method has inherent limitations. The conventional Adam optimizer provides fast local convergence through adaptive learning rates and momentum estimation, but as a gradient-based local search method it may become trapped in local minima when applied to multimodal objective functions (Kingma & Ba, 2015). PSO offers effective global exploration through particle interactions, but it is prone to premature convergence and loss of population diversity (Poli et al., 2007). GWO maintains a balance between exploration and exploitation using hierarchical search agents, yet it does not incorporate adaptive gradient information that can accelerate local refinement (Mirjalili et al., 2014).

The Adam Gradient Descent Optimizer (AGDO) is a recent advancement in optimization algorithms that builds on the Adam algorithm by integrating gradient momentum with a global search mechanism. This combination enables a more effective balance between exploration and exploitation, potentially increasing convergence speed and reducing the risk of becoming trapped in local minima (Xia & Ji, 2025). Compared with many methods of metaheuristic optimization, AGDO employs relatively simple mathematical formulations and does not require extensive hyperparameter tuning. In practical applications, the algorithm mainly relies on standard settings such as population size and maximum iteration number, while the remaining adaptive parameters follow the default configuration inherited from the Adam optimization framework. These characteristics make AGDO relatively easy to implement and computationally efficient for nonlinear optimization problems.

Despite its potential, the application of AGDO in geophysical inversion problems, particularly in magnetotelluric (MT) inversion, remains limited. To the authors' knowledge, the implementation of AGDO for one-dimensional MT inversion has not been widely reported in the literature. Therefore, this study implements the AGDO algorithm for one-dimensional MT data inversion and evaluates its performance in reconstructing subsurface resistivity models using both synthetic and field data. The objective is to assess the algorithm's ability to produce model solutions consistent with observational data.

2. METHODS

A numerical modeling approach was employed to evaluate the effectiveness of the AGDO algorithm in addressing one-dimensional inversion problems of MT data. The research proceeded through several sequential stages. Initially, the AGDO algorithm was tested using the peaks function,

a simple benchmark, to assess its ability to identify global solutions on complex function surfaces and avoid convergence to local minima. Following verification of the algorithm's optimization capability, it was applied to synthetic MT data generated from a layered Earth model to evaluate inversion accuracy under controlled conditions. In the final stage, the AGDO algorithm was applied to field MT data to assess its performance on more complex, realistic datasets. This workflow demonstrates the progression from algorithm testing to practical application in MT inversion.

2.1 Magnetotelluric (MT) Forward and Inverse Modelling

The MT response of a layered Earth model is characterized by an impedance tensor (**Z**) that links the horizontal electric field (**E**) and horizontal magnetic field (**H**) components. This relationship is expressed as Equation 1 (Vozoff, 1990).

$$\mathrm{E} = \mathrm{Z}\,\mathrm{H} \tag{1}$$

In a 1–D layered Earth model, the MT response can be calculated through forward modelling using a recursive impedance formulation. The intrinsic impedance of a homogeneous layer is expressed as Equation 2.

$$Z_{0j} = \sqrt{i\omega\mu_0\rho_j} \tag{2}$$

where Z_{0j} is the intrinsic impedance of the j-th layer, i is the imaginary unit, ω is the angular frequency of the electromagnetic field, μ_0 is the magnetic permeability of free space, and ρ_j is the electrical resistivity of the j-th layer.

The reflection coefficient between two successive layers is defined as Equation 3.

$$R_j = \frac{Z_{j+1} - Z_{0j}}{Z_{j+1} + Z_{0j}} \tag{3}$$

where R_j is the reflection coefficient between the j-th layer and the underlying $(j+1)$-th layer, Z_{j+1} is the impedance of the lower layer, and Z_{0j} is the intrinsic impedance of the j-th layer.

The impedance of the j-th layer can then be calculated recursively as Equation 4.

$$Z_j = Z_{0j}\frac{1 - R_j e^{-2h_j/Z_{0j}}}{1 + R_j e^{-2h_j/Z_{0j}}} \tag{4}$$

where Z_j is the impedance at the top of the j-th layer, h_j represents the thickness of the j-th layer, and e denotes the exponential function.

Based on these impedance values, the observation parameters in MT, namely apparent resistivity and phase, can be calculated using Equations 5 and 6.

$$\rho_a = \frac{1}{\omega\mu_0}|Z_1|^2 \tag{5}$$

$$\phi = tan^{-1}\left(\frac{\mathrm{Im}(Z)}{\mathrm{Re}(Z)}\right) \tag{6}$$

Where ρ_a is the apparent resistivity, ω is the angular frequency, and μ_0 is the magnetic permeability, $\mathrm{Im}(Z)$ represents the imaginary part of the impedance, and $\mathrm{Re}(Z)$ represents the real part of the impedance (Grandis & Maulana, 2017). In this study, forward modelling was used to calculate the theoretical magnetotelluric (MT) response of a layered Earth model in the form of apparent resistivity and phase curves as a function of period (Wang et al., 2023).

Instead, the inverse modelling process aims to estimate subsurface resistivity parameters by minimizing the difference between observational data and modeled responses. The objective function used in this study is the root mean square error (RMSE), which measures the misfit between observed and calculated apparent resistivity and phase responses, as expressed in Equation 7.

$$RMSE = \sqrt{\frac{1}{N}\sum_{i=1}^{N}\left[\left(\log_{10}\frac{\rho_{a,i}^{obs}}{\rho_{a,i}^{cal}}\right)^2 + \left(\phi_i^{obs} - \phi_i^{cal}\right)^2\right]} \quad (7)$$

N :Number of data points
$\rho_{a,i}^{obs}$ & $\rho_{a,i}^{cal}$:Observed and calculated apparent resistivity
ϕ_i^{obs} & ϕ_i^{cal} :Observed and calculated phase

The apparent resistivity term is evaluated in logarithmic space to account for the wide dynamic range commonly observed in MT data. Following common practice in magnetotelluric inversion, apparent resistivity and phase are jointly incorporated into a single objective function because they provide complementary information about subsurface resistivity structures (Baba & Chave, 2005). Although they represent different physical quantities, the logarithmic resistivity ratio and phase difference expressed in radians are dimensionless, allowing them to be combined within a unified RMSE formulation. The objective function is then minimized to obtain the resistivity model that best fits the observed MT data.

2.2 Adam Gradient Descent Optimizer (AGDO)

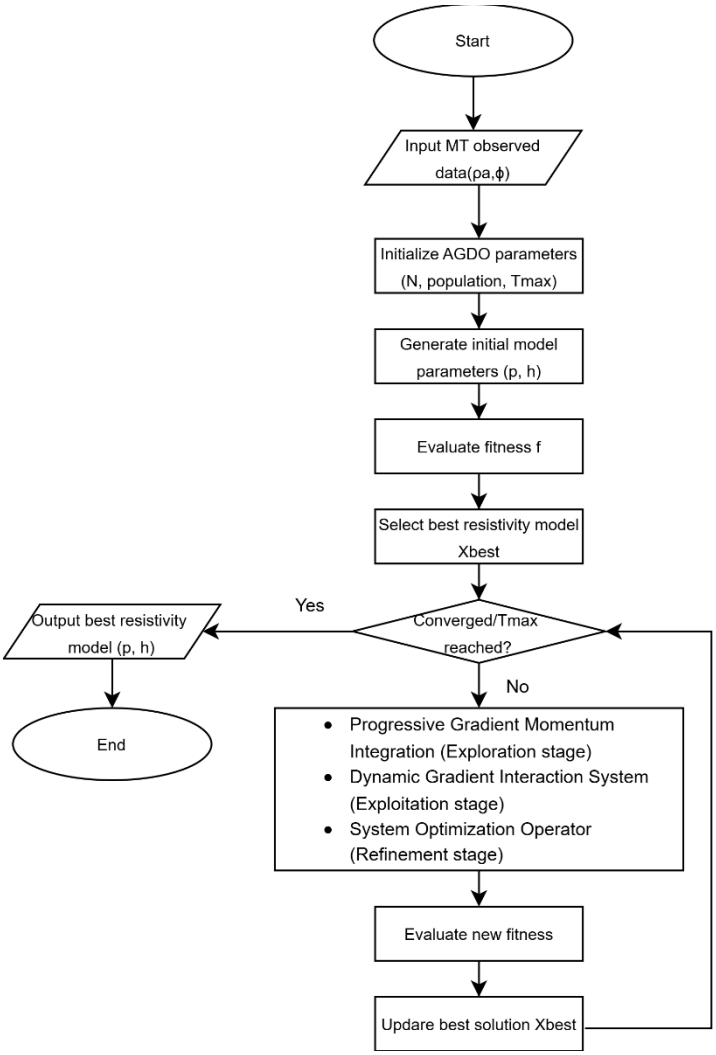


Figure 1. Workflow of the Adam Gradient Descent Optimizer (AGDO) algorithm for magnetotelluric (MT) inversion

The optimization process in this study was implemented using the AGDO algorithm. This algorithm operates by utilizing a set of candidate solutions that are iteratively updated in the search space to find the optimal solution of the objective function (Xia & Ji, 2025).

In the AGDO algorithm, each individual in the population represents a candidate solution in the parameter space. The search direction used to guide the i-th solution at iteration t is defined by the interaction between the current best solution and the population distribution, as expressed in Equation (8).

$$g_i^t = X_{best}^t - CP \tag{8}$$

where g_i^t represents the search direction of the i-th solution at iteration t, $X_{best}^t$is the current best solution in the population, C is a stochastic adjustment factor within the range [0, 1], and P represents the interaction term that reflects the relative position of the current solution with respect to the population distribution. This formulation guides candidate solutions toward promising regions of the search space while maintaining population diversity during the optimization process.

To maintain the stability of the search direction during the iteration process, the gradient momentum is calculated using Equation 9.

$$m_i^{t+1} = \beta m_i^{t-1} + (1-\beta) g_i^t \tag{9}$$

where m_i^{t+1} represents the gradient momentum of the i-th solution at iteration $t+1$, m_i^{t-1} is the momentum from the previous iteration, and β is the momentum coefficient that controls the influence of previous gradients. The momentum component helps preserve the search direction from previous iterations, thereby reducing oscillatory updates during optimization. This mechanism improves convergence stability and accelerates the search toward promising regions of the model space.

In addition to utilizing gradients, AGDO also calculates the interactions between solutions in the population shown in Equation 10.

$$I_i^t = \sum_{j \neq i} w_{ij} \left(x_j^t - x_i^t \right) \tag{10}$$

where I_i^t represents the interaction term between candidate solutions, and x_i^t and x_j^t denote the positions of the i-th and j-th solutions in the search space, and w_{ij} is the interaction weight that controls the influence of neighboring solutions. The interaction term introduces information exchange among candidate solutions in the population. Through this mechanism, each solution is influenced not only by its own gradient information but also by the positions of neighboring solutions. This interaction enhances global exploration capability and reduces the likelihood of premature convergence to local minima.

The solution update vector is obtained from the combination of the gradient momentum and interaction components as stated in Equation 11.

$$u_i^{t+1} = m_i^{t+1} + \alpha I_i^t \tag{11}$$

where u_i^{t+1} represents the update vector of the i-th solution at iteration $t+1$, and α is a weighting parameter controlling the contribution of the interaction term.

Next, the solution position is updated using Equation 12.

$$x_i^{t+1} = x_i^t + \eta u_i^t \tag{12}$$

where x_i^{t+1} represents the updated position of the i-th solution at iteration $t+1$, x_i^t denotes the position of the solution at iteration t, u_i^t represents the update vector obtained from Equation 11, and η is the learning rate parameter that controls the step size of the optimization process. By combining adaptive gradient updates and population interactions, AGDO balances exploitation and exploration during the optimization process. This balance is important for MT inversion problems,

which commonly exhibit nonlinear and non-unique characteristics. The iteration process continues until the convergence criteria are met or the maximum number of iterations is reached. In this study, convergence was evaluated based on the improvement of the best objective function value between successive iterations. The optimization process was terminated when the absolute improvement of the best misfit value remained smaller than 10^{-3} for 25 consecutive iterations. The patience value of 25 was selected empirically to allow sufficient exploration of the model space and to avoid terminating the optimization during temporary stagnation. Smaller patience values may restrict the global search process and increase the likelihood of premature convergence. This stopping criterion was implemented to prevent unnecessary computations after the optimization had reached a stable solution while reducing the risk of premature termination.

2.3 Synthetic Model

The Adam Gradient Descent Optimizer (AGDO) algorithm was tested by inverting synthetic data generated from a one-dimensional layered Earth model. The model consisted of three homogeneous layers with specific resistivity and thickness parameters, while the deepest layer was assumed to be a half-space with infinite thickness. Four synthetic models with different resistivity configurations were designed to evaluate the capability of the AGDO algorithm. Models 1 and 2 represent simple three-layer structures, whereas Models 3 and 4 represent more complex four-layer structures with additional resistivity interfaces, allowing further evaluation of the algorithm under increased model complexity. These models were selected to assess the robustness, stability, and resolution capability of the inversion algorithm under different subsurface resistivity distributions commonly encountered in magnetotelluric (MT) problems.

Tabel 1. Synthetic model parameters for testing the AGDO algorithm in 1D magnetotelluric (MT) inversion

Layer	Model 1		Model 2		Model 3		Model 4	
	Resistivity ($\Omega\, m$)	Thickness (m)	Resistivity ($\Omega\, m$)	Thickness (m)	Resistivity ($\Omega\, m$)	Thickness (m)	Resistivity ($\Omega\, m$)	Thickness (m)
1	100	500	100	500	100	500	100	500
2	1000	1000	10	1000	1500	250	20	500
3	10	-	1000	-	20	1000	500	1000
4	-	-	-	-	1000	-	1000	-

The response of synthetic data in form of apparent resistivity and phase was calculated using one-dimensional forward modelling in a logarithmic frequency range of 10^{-3} to 10^{4} Hz with 56 frequency points. To simulate realistic field measurement conditions, 5% Gaussian noise was added to the complex impedance before recalculating the apparent resistivity and phase responses (Muttaqien & Nurjaman, 2021). In practical MT surveys, electromagnetic responses are commonly contaminated by environmental and instrumental noise. Therefore, the addition of 5% Gaussian noise was considered sufficient to represent realistic observational uncertainty while allowing evaluation of the inversion algorithm performance under noisy conditions. The noisy synthetic data also enabled assessment of the stability and consistency of the AGDO algorithm under imperfect observational conditions. The noisy impedance can be expressed as Equation 13.

$$Z_{noise} = Z(1 + \epsilon_r) + iZ_{\epsilon_i} \tag{13}$$

where Z represents the original impedance value, Z_{noise} denotes the impedance after noise addition, and ϵ_r and ϵ_i are random variables following a Gaussian distribution corresponding to the selected noise level.

The number of inversion parameters depends on the synthetic model configuration. For Models 1 and 2, the inversion estimates three resistivity values and two-layer thicknesses, resulting in five unknown parameters. For Models 3 and 4, four resistivity values and three-layer thicknesses are estimated, resulting in seven unknown parameters. The increase in parameter number expands the search space and provides a more rigorous assessment of the AGDO algorithm under more

complex inversion conditions. In synthetic data tests, the model space was limited to a resistivity range of 1–3000 Ωm and a layer thickness of 1–2000 m. The parameter bounds were selected to encompass the true model parameters while remaining sufficiently broad to avoid biasing the inversion process. For field data, the model space limits were determined more specifically for each layer to maintain the model's suitability to the characteristics of the observed data.

For the synthetic data inversion, the AGDO algorithm was implemented using a population size of 120 and a maximum iteration number of 150. The optimization process employed Adam adaptive parameters with $\beta_1 = 0.9$, $\beta_2 = 0.999$, and a learning rate of 0.05. These parameter settings were selected empirically through preliminary numerical experiments and were considered sufficient to achieve stable convergence for the synthetic layered models. The relatively larger population size was used to improve exploration of the model space and to enhance the consistency of inversion results across repeated runs.

Due to the stochastic nature of the AGDO algorithm, the inversion process was executed repeatedly to ensure the stability of the solution obtained. In this study, the inversion program was run 100 times, resulting in 100 candidate resistivity models generated from different random initial populations. Each run produced a model with a corresponding misfit value. The final resistivity model was selected based on the minimum misfit obtained among all runs.

2.4 Field Magnetotelluric (MT) Data

After evaluating the performance of the AGDO algorithm using synthetic data, the method was subsequently applied to field MT data to assess its capability under real geological conditions. In this study, the AGDO algorithm was used to invert MT data from the Cloncurry region, Queensland, Australia. The dataset is publicly available and published by Geoscience Australia as part of the Cloncurry regional MT survey (PID: https://pid.geoscience.gov.au/dataset/ga/110141). The Cloncurry region is part of the Mount Isa mineral province, which is characterized by complex Proterozoic geological formations and significant copper-gold mineralization systems. Regional MT investigations in this area were conducted to image subsurface resistivity structures, improve understanding of crustal architecture, and support regional mineral exploration programs. The data consists of frequency-dependent apparent resistivity and phase responses derived from MT measurements.

The subsurface model parameters estimated during the inversion consisted of resistivity values and layer thicknesses, with the number of layers varying between stations according to the complexity of the observed MT data. Stations exhibiting relatively simple apparent resistivity and phase characteristics were represented using four-layer models, whereas stations with more complex responses were represented using five-layer models to adequately capture the main subsurface resistivity variations while maintaining inversion stability and computational efficiency. The inversion search space was generally constrained to resistivity values ranging from 1 to 20,000 Ωm and layer thicknesses ranging from 1 to 50,000 m. These parameter bounds were subsequently refined for each station based on the characteristics of the apparent resistivity and phase curves to ensure geologically plausible solutions while maintaining an efficient and stable inversion process.

For the field MT inversion, the AGDO algorithm employed a population size of 200 and a maximum iteration number of 300 to improve exploration within the more complex model space associated with real observational data. The optimization utilized Adam adaptive parameters with $\beta_1 = 0.9$ and $\beta_2 = 0.999$, while the learning rate was adaptively decreased during the iteration process. These parameter settings were selected empirically through preliminary numerical experiments to obtain stable convergence and consistent inversion results for the field dataset.

The inversion procedure applied to the field data followed the same computational framework used in the synthetic model experiments. Due to the stochastic nature of the AGDO algorithm, the inversion was executed repeatedly with different initial populations, and the final resistivity model was selected based on the minimum misfit value obtained among the inversion runs. To support reproducibility and further research development, the implementation code of the AGDO algorithm used for the synthetic and field MT inversion experiments in this study is publicly available at: https://github.com/alyasirharahap/AGDO-MT-Inversion.

3. RESULT AND DISCUSSION

3.1 Performance of AGDO on Peaks Function

The optimization performance of AGDO was evaluated using the peaks benchmark function. As illustrated in Figure 2, the candidate solutions are initially scattered across the search space and gradually move toward the region of the global optimum as the iterations increase. The population distribution becomes increasingly concentrated around the optimal point, indicating the transition from exploration to exploitation during the optimization process. At the 100th iteration, most solutions converge near the optimum position with a best misfit value of approximately 1.8938. These results demonstrate that AGDO is capable of effectively exploring the search space and achieving stable convergence toward the optimal solution. This behavior indicates that the algorithm maintains a good balance between exploration and exploitation during the optimization process.

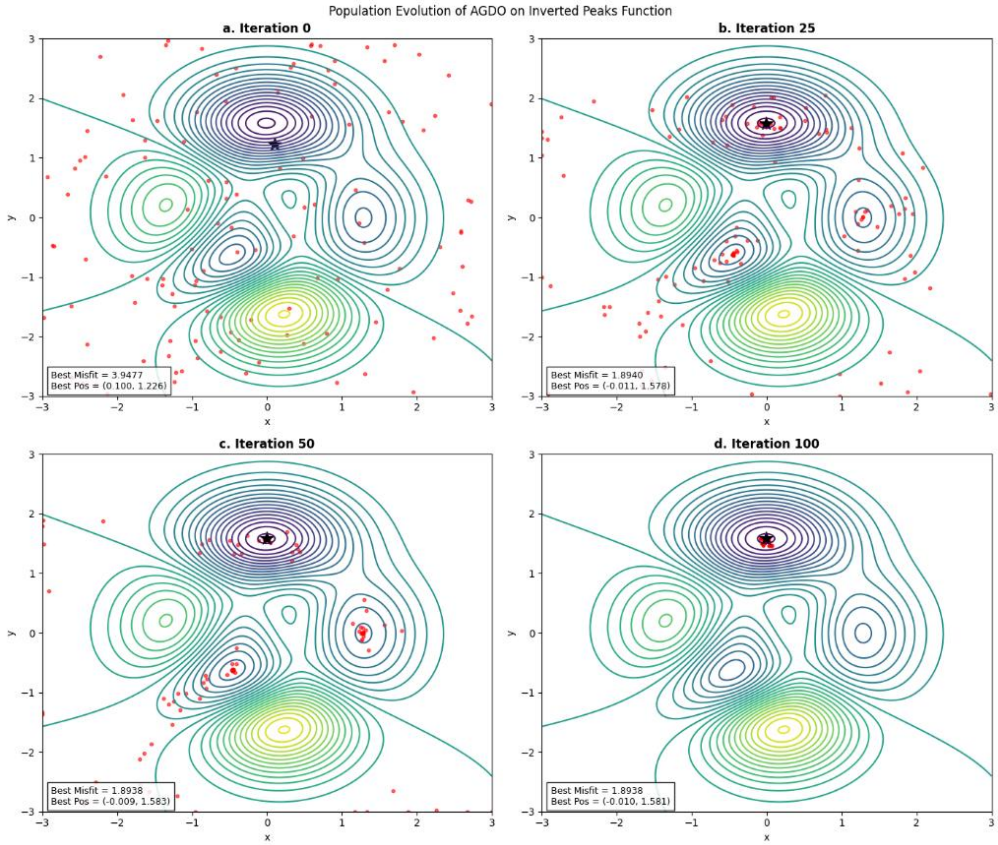


Figure 2. Population evolution of the AGDO algorithm on the inverted Peaks benchmark function. The red dots represent candidate solutions, and the black star indicates the best solution at each iteration: (a) iteration 0, (b) iteration 25, (c) iteration 50, and (d) iteration 100

3.2 Synthetic Data Inversion

The results of synthetic data inversion using the AGDO algorithm are shown in Figures 3–6. Subplots (a) and (b) present a comparison between synthetic data and calculated responses for apparent resistivity and phase as a function of period. The blue dots represent synthetic data with added noise, while the red lines represent responses calculated from the inversion model. The calculated curves follow the pattern of the synthetic data across the entire period range, indicating a good agreement between observed and calculated responses. This agreement suggests that the inversion model is capable of accurately reproducing the MT responses of the synthetic data. The variation of apparent resistivity with increasing period reflects the response of different subsurface layers, where shorter periods represent shallow structures and longer periods correspond to deeper resistivity contrasts.

The resistivity model obtained from the inversion is shown in subplot (c). The blue line represents the synthetic model used as a reference, while the red dashed line shows the best model obtained from the inversion process using the AGDO algorithm. The inversion results demonstrate

that AGDO can accurately reconstruct both simple three-layer models and more complex four-layer models while maintaining stable convergence behavior. The successful reconstruction of Models 3 and 4 indicates that AGDO remains effective even when the number of inversion parameters increases and additional resistivity interfaces are introduced.

Besides the best model, subplot (c) also displays a set of inversion models obtained from 100 independent runs, shown by the gray lines. The distribution of these models shows that most solutions are clustered around the best model. This indicates that the optimization process carried out by the AGDO algorithm produces consistent solutions even when the inversion starts from different initial populations. This clustering behavior demonstrates the stability and reliability of the optimization process across repeated runs.

The best RMSE values obtained for Models 1–4 range from approximately 0.0599 to 0.0603, indicating consistent inversion performance even as the number of model parameters increases. The close agreement between the best and mean RMSE values further demonstrates the stability of the inversion results across repeated runs. These values indicate that the responses calculated from the inversion model are in good agreement with the synthetic data. The convergence behavior of the algorithm is illustrated by the convergence curves in Figure 7 for all four synthetic models. Although the initial misfit values differ due to random population initialization and variations in model complexity, all models exhibit a rapid decrease in misfit during the early iterations and converge toward stable solutions with RMSE values of approximately 0.06. This behavior indicates that the AGDO algorithm efficiently explores the solution space during the early stage of the optimization process and subsequently refine the model parameters until a stable solution is obtained.

In addition to producing stable inversion results, the AGDO algorithm demonstrated relatively efficient computational performance during the synthetic inversion experiments. Based on the implementation used in this study, a single inversion run required approximately 20 seconds on a laptop equipped with an AMD Ryzen 5 7535HS processor, 16 GB RAM, and an NVIDIA GeForce RTX 3050 Laptop GPU. The relatively short computation time is advantageous for repeated inversion runs and stability analyses involving multiple random initial populations. These results indicate that AGDO can be practically implemented for one-dimensional MT inversion problems using moderate computational resources.

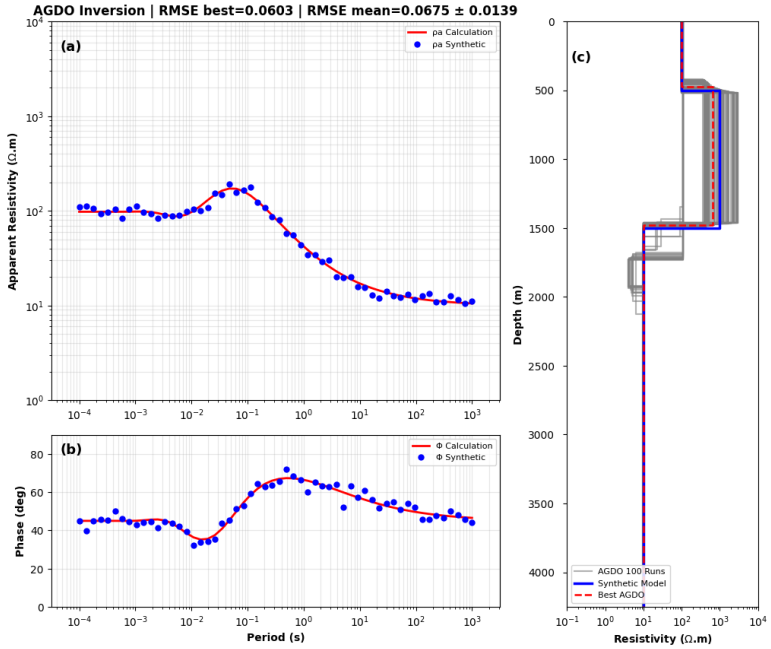


Figure 3. Synthetic inversion results for Model 1 using the AGDO algorithm. (a) Comparison between synthetic and calculated apparent resistivity curves. (b) Comparison between synthetic and calculated phase responses. (c) Comparison between the synthetic resistivity model (blue), the best inversion model obtained by AGDO (red dashed line), and the ensemble of models from 100 independent runs (gray).

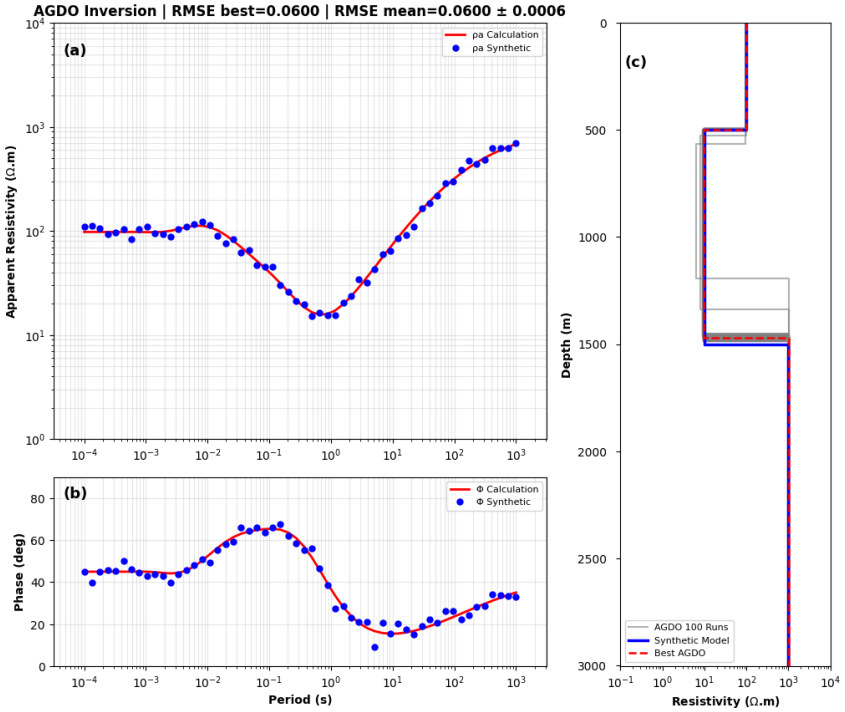


Figure 4. Synthetic inversion results for Model 2 using the AGDO algorithm. (a) Comparison between synthetic and calculated apparent resistivity curves. (b) Comparison between synthetic and calculated phase responses. (c) Comparison between the synthetic resistivity model (blue), the best inversion model obtained by AGDO (red dashed line), and the ensemble of models from 100 independent runs (gray).

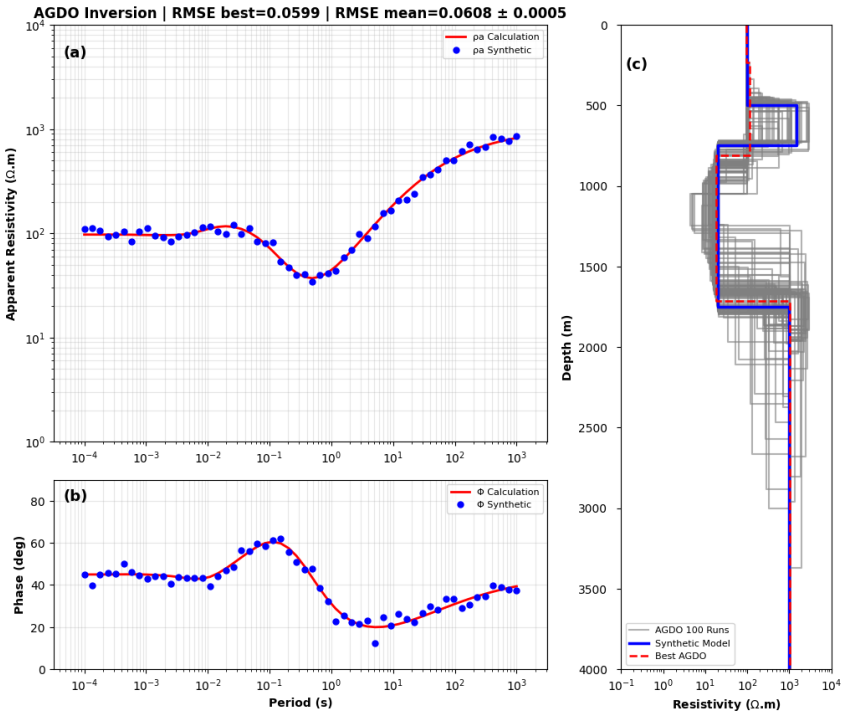


Figure 5. Synthetic inversion results for Model 3 using the AGDO algorithm. (a) Comparison between synthetic and calculated apparent resistivity curves. (b) Comparison between synthetic and calculated phase responses. (c) Comparison between the synthetic resistivity model (blue), the best inversion model obtained by AGDO (red dashed line), and the ensemble of models from 100 independent runs (gray).

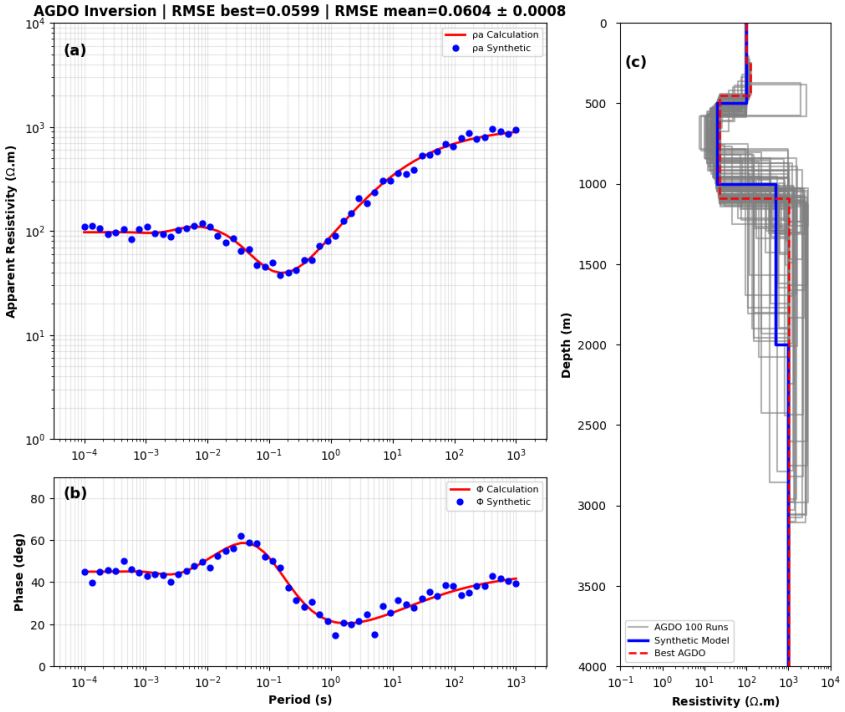


Figure 6. Synthetic inversion results for Model 4 using the AGDO algorithm. (a) Comparison between synthetic and calculated apparent resistivity curves. (b) Comparison between synthetic and calculated phase responses. (c) Comparison between the synthetic resistivity model (blue), the best inversion model obtained by AGDO (red dashed line), and the ensemble of models from 100 independent runs (gray).

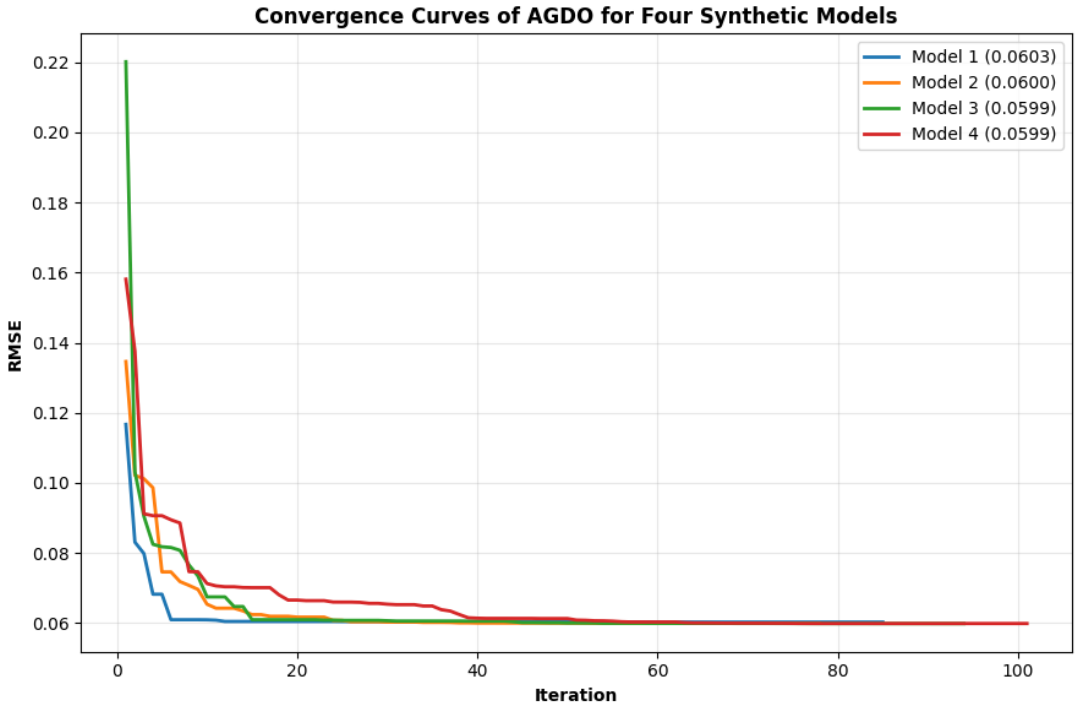


Figure 7. Convergence curves of AGDO for the four synthetic models, showing the decrease of misfit values with increasing iterations during the inversion process.

3.3 Magnetotelluric (MT) Field Data Inversion

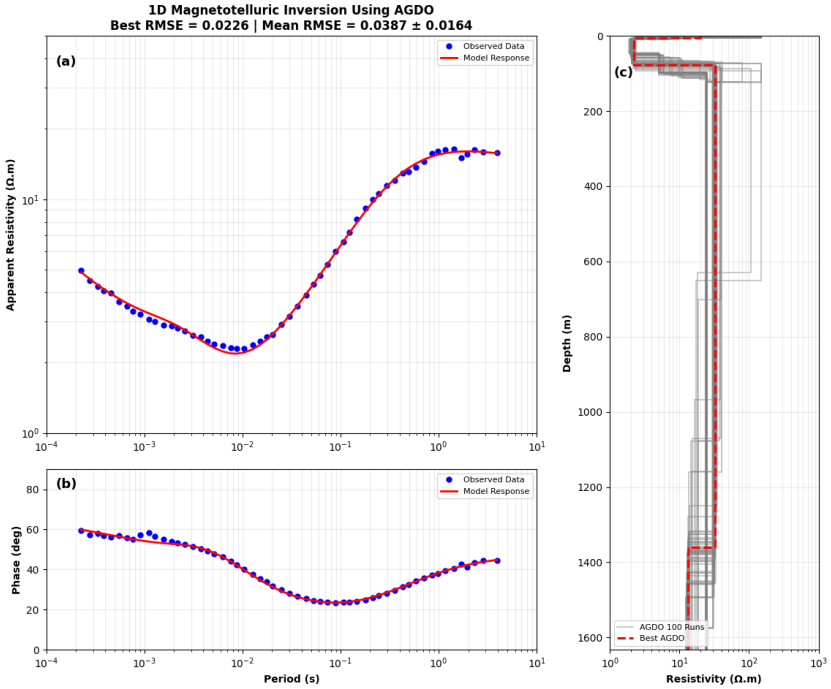


Figure 8. Field magnetotelluric (MT) inversion results at station L02S18 using the AGDO algorithm. (a) Comparison between observed and calculated apparent resistivity curves. (b) Comparison between observed and calculated phase responses. (c) Resistivity model showing the best inversion result obtained by AGDO (red dashed line), and the ensemble of models from 100 independent runs (gray lines).

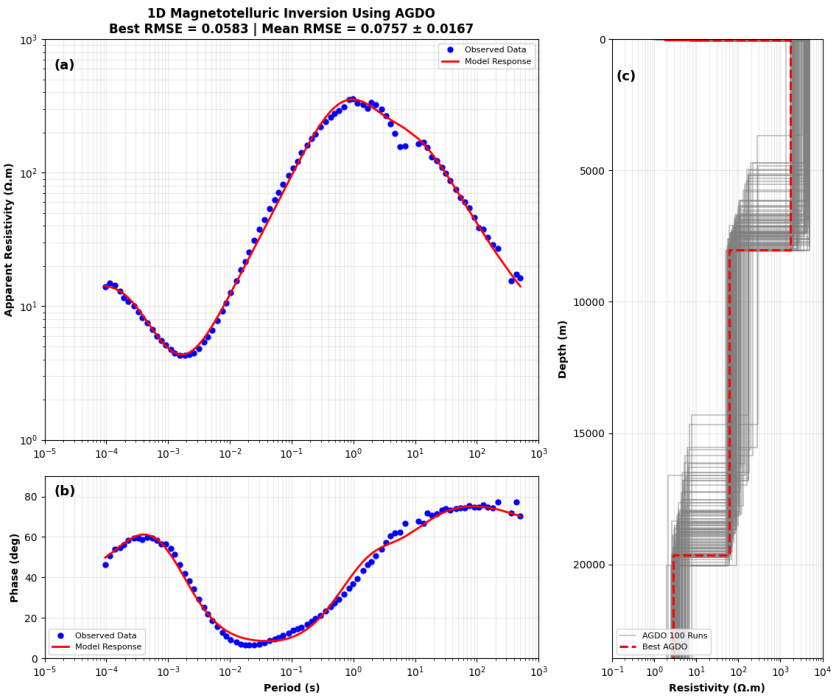


Figure 9. Field magnetotelluric (MT) inversion results at station L19S12 using the AGDO algorithm. (a) Comparison between observed and calculated apparent resistivity curves. (b) Comparison between observed and calculated phase responses. (c) Resistivity model showing the best inversion result obtained by AGDO (red dashed line), and the ensemble of models from 100 independent runs (gray lines).

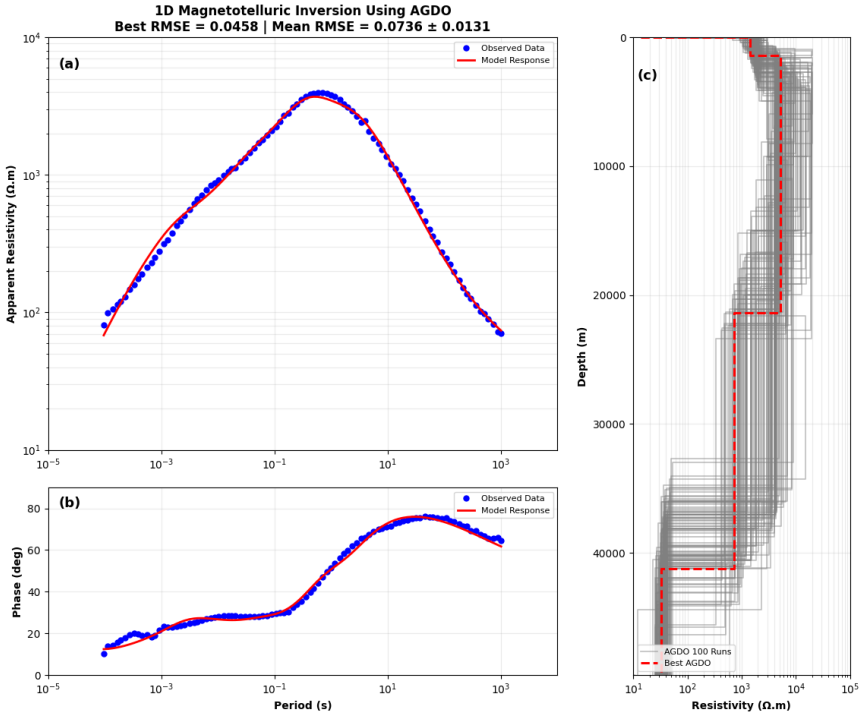


Figure 10. Field magnetotelluric (MT) inversion results at station L19S10 using the AGDO algorithm. (a) Comparison between observed and calculated apparent resistivity curves. (b) Comparison between observed and calculated phase responses. (c) Resistivity model showing the best inversion result obtained by AGDO (red dashed line), and the ensemble of models from 100 independent runs (gray lines).

The inversion results of field MT data using the AGDO algorithm at three measurement points (L02S18, L19S12, and L19S10) demonstrate consistent and stable performance. As shown in Figure 8–10, the calculated responses exhibit good agreement with the observed data for both apparent resistivity and phase across the entire period range. This agreement indicates that the inversion models can adequately represent the measured MT responses.

The obtained misfit values are relatively low, with best RMSE values of 0.0225 for L02S18, 0.0582 for L19S12, and 0.0464 for L19S10. The mean misfit values are close to the best values and are accompanied by relatively small standard deviations. This indicates that the inversion results are consistent across repeated runs with different random initial populations.

The stability of the inversion is further supported by the distribution of models from 100 independent runs (Figure 8–10 (c)), where most models cluster around the best solution, particularly at shallow to intermediate depths. This clustering behavior demonstrates that the AGDO algorithm consistently converges toward similar solutions despite different initial conditions, indicating a high level of reliability in the inversion results.

Although greater variability is observed at deeper depths, this behavior is expected due to the decreasing sensitivity of MT data with depth and the inherent non-uniqueness of the inversion problem (Desifatma et al., 2024; Spies, 1989). Importantly, this variability does not significantly affect the main resistivity structure, which remains consistent across multiple runs.

The inverted resistivity models provide a general representation of the subsurface resistivity structure in the Cloncurry region. Relatively low-resistivity zones may be associated with conductive sedimentary sequences, alteration zones, or fluid-rich structures, whereas higher resistivity layers likely represent crystalline basement rocks or more resistive geological formations. This interpretation is consistent with the geological characteristics of the Cloncurry region, which forms part of the Mount Isa mineral province and is known for complex Proterozoic basement structures and significant copper-gold mineralization systems. Regional magnetotelluric investigations in this area are commonly conducted to image basement architecture and identify subsurface structures associated with mineral exploration targets.

Compared to conventional deterministic inversion methods that typically produce a single solution, the AGDO-based approach provides an ensemble of models that allows for the evaluation of solutions consistency and uncertainty. This represents an important advantage in interpreting subsurface structures, particularly under complex geological conditions. Overall, the results demonstrate that the AGDO algorithm can provide robust, stable, and consistent inversion results for field MT data.

4. CONCLUSION

The implementation of the Adam Gradient Descent Optimizer (AGDO) for one-dimensional (1-D) magnetotelluric (MT) inversion has been successfully carried out using both synthetic and field datasets. The results indicate that AGDO is capable of reconstructing subsurface resistivity structures under nonlinear and non-unique inversion conditions while maintaining stable convergence behavior across repeated inversion runs.

The application to field data demonstrates that AGDO can produce reliable inversion models with good agreement between the observed and calculated MT responses. The consistency of the solutions obtained from repeated runs indicates that AGDO converges toward similar subsurface resistivity structures despite different random initial populations, highlighting the stability of the inversion process. Furthermore, the successful reconstruction of both simple and more complex synthetic models confirms the capability of AGDO to handle varying levels of model complexity in MT inversion problems.

An important contribution of this study is the implementation of a relatively recent optimization algorithm for magnetotelluric inversion, particularly in one-dimensional MT modelling. Compared with many population-based optimization methods, AGDO employs relatively simple mathematical formulations and requires only limited parameter adjustment, making the algorithm easier to implement for practical inversion applications. In addition, the computational performance observed during the inversion experiments indicates that AGDO can be effectively applied using moderate computational resources.

Future studies may further evaluate the performance of AGDO through comparative analyses with other optimization algorithms and extend its implementation to more complex MT inversion problems, including two-dimensional and three-dimensional modelling. In addition, the promising results obtained in this study suggest that AGDO has potential for application to other one-dimensional geophysical inversion problems characterized by nonlinear and non-unique solution spaces, such as Horizontal-to-Vertical Spectral Ratio (HVSR), Multichannel Analysis of Surface Waves (MASW), and vertical electrical sounding (VES) inversion.

ACKNOWLEDGEMENTS

The authors would like to express their gratitude to the Geophysical Engineering Study Program, Faculty of Industrial Technology, Institut Teknologi Sumatera (ITERA), for the support provided during this research. The authors also acknowledge Geoscience Australia for providing the magnetotelluric (MT) dataset used in this study.

REFERENCES

Baba, K., & Chave, A. D. (2005). Correction of seafloor magnetotelluric data for topographic effects during inversion. *Journal of Geophysical Research: Solid Earth*, *110*(12), 1–16. https://doi.org/10.1029/2004JB003463

Chave, A. D., & Jones, A. G. (2021). *The Magnetotelluric Method: Theory and Practice* (Vol. 32, Issue 3).

Constable, S. C., Parker, R. L., & Constable, C. G. (1987). Occam's inversion: a practical algorithm for generating smooth models from electromagnetic sounding data. *Geophysics*, *52*(3), 289–300. https://doi.org/10.1190/1.1442303

Dell'aversana, P. (2023). Inversion of geophysical data supported by Reinforcement Learning. *Bulletin of Geophysics and Oceanography*, *64*(1), 45–60. https://doi.org/10.4430/bgo00411

Desifatma, E., Djaja, I. G. P. F. S., Pratomo, P. M., Supriyadi, Mustopa, E. J., Evita, M., Djamal, M., & Srigutomo, W. (2024). Robust inversion of 1D magnetotelluric data using the Huber loss

function. *Computational Geosciences*, *28*(4), 629–643. https://doi.org/10.1007/s10596-024-10286-x

Goyes-Peñafiel, P., Bin Waheed, U., & Arguello, H. (2025). Physically Guided Deep Unsupervised Inversion for 1-D Magnetotelluric Models. *IEEE Geoscience and Remote Sensing Letters*, *22*, 1–5. https://doi.org/10.1109/LGRS.2025.3528767

Grandis, H. (1999). An alternative algorithm for one-dimensional magnetotelluric response calculation. *Computers and Geosciences*, *25*(2), 119–125. https://doi.org/10.1016/S0098-3004(98)00110-1

Grandis, H., & Maulana, Y. (2017). Particle Swarm Optimization (PSO) for Magnetotelluric (MT) 1D Inversion Modeling. *IOP Conference Series: Earth and Environmental Science*, *62*(1). https://doi.org/10.1088/1755-1315/62/1/012033

Hu, X., Bai, N., Han, B., Peng, R., Zhou, J., Zhu, D., & Huang, G. (2025). 3D inversion algorithm of magnetotelluric data based on the solution equivalence constrain. *Geophysics*, *90*(3), E91–E104. https://doi.org/https://doi.org/10.1190/geo2024-0252.1

Junian, W. E., Adilla, R. P., & Irawati, S. M. (2025). Implementasi Algoritma Grey Wolf Optimizer (GWO) Untuk Pemodelan Inversi 1D Data Magnetotellurik. *Jurnal Geosaintek*, *11*(2), 197–206. https://doi.org/10.12962/j25023659.v11i2.2590

Junian, W. E., Grandis, H. (2023). Hybrid Particle Swarm Optimization and Grey Wolf Optimizer Algorithm For Controlled Source Audio- Frequency Magnetotellurics (CSAMT) One-Dimensional Inversion Modelling. Rudarsko-geološko-naftni zbornik, 38 (3), 65-80. https://doi.org/ 10.17794/rgn.2023.3.6

Junian, W. E., Styawan, Y., Prasetyo, N., Paembonan, A. Y. (2026). Applying the One-to-One-Based Optimizer (OOBO) Algorithm for One-Dimensional Inversion Modeling of Magnetotellurics Data. *Pure Appl. Geophys.* https://doi.org/10.1007/ s00024-026-03998-x

Kingma, D. P., & Ba, J. L. (2015). Adam: A method for stochastic optimization. *3rd International Conference on Learning Representations, ICLR 2015 - Conference Track Proceedings*, 1–15. https://doi.org/https://doi.org/10.48550/arXiv.1412.6980

Li, F., Wang, P., & Lu, K. (2026). Gauss-Newton inversion of ground transient electromagnetic data using COMSOL multiphysics. *Scientific Reports*, *16*(1), 1–13. https://doi.org/10.1038/s41598-025-30438-y

Liu, W., Wang, H., Xi, Z., Zhang, R., & Huang, X. (2022). Physics-Driven Deep Learning Inversion with Application to Magnetotelluric. *Remote Sensing*, *14*(13). https://doi.org/10.3390/rs14133218

Mirjalili, S., Mohammad, S., & Lewis, A. (2014). Advances in Engineering Software Grey Wolf Optimizer. *Advances in Engineering Software*, *69*, 46–61. https://doi.org/10.1016/j.advengsoft.2013.12.007

Mukesh, Sarkar, K., & Singh, U. K. (2023). The joint application of a metaheuristic algorithm and a Bayesian statistics approach for uncertainty and stability assessment of nonlinear magnetotelluric data. *Nonlinear Processes in Geophysics*, *30*(4), 435–456. https://doi.org/10.5194/npg-30-435-2023

Muttaqien, I., & Nurjaman, J. (2021). Two-dimensional inversion modeling of magnetotelluric (MT) synthetic data of a graben structure using SimPEG. *Riset Geologi Dan Pertambangan*, *31*(1), 1–12. https://doi.org/10.14203/risetgeotam2021.v31.1121

Oryński, S., Jóźwiak, W., Nowożyński, K., & Klityński, W. (2022). Comparison of 3D, 2D, and 1D Magnetotelluric Inversion Results on the Example of Data from Fore-Sudetic Monocline. *International Journal of Geophysics*, *2022*.

Parker, R. L. (1983). The magnetotelluric inverse problem. *Most*, *6*, 5–25.

Pedersen, J., & Hermance, J. F. (1986). Least squares inversion of one-dimensional magnetotelluric data: An assessment of procedures employed by Brown University. *Surveys in Geophysics*, *8*(2), 187–231. https://doi.org/10.1007/BF01902413

Poli, R., Kennedy, J., & Blackwell, T. (2007). Quantification & Assessment of the chemical form of residual gadolinium in the brain.pdf. *Swarm Intell*, *1*, 33–57. https://doi.org/10.1007/s11721-007-0002-0

Rodi, W., & Mackie, R. L. (2001). Nonlinear conjugate gradients algorithm for 1D magnetotelluric inversion. *Geophysical Prospecting for Petroleum*, *66*(1), 174–187. https://doi.org/10.3969/j.issn.1000-1441.2014.06.017

Simpson, F., & Bahr, K. (1997). Practical Magnetotellurics. *Geophysical Journal International*.

Siripunvaraporn, W. (2012). Three-Dimensional Magnetotelluric Inversion: An Introductory Guide for Developers and Users. *Surveys in Geophysics*, *33*(1), 5–27. https://doi.org/10.1007/s10712-011-9122-6

Spies, B. R. (1989). Depth of investigation in electromagnetic sounding methods. *Geophysics*, *54*(7), 872–888. https://doi.org/10.1190/1.1442716

Syaripudin, A., & Grandis, H. (2001). *Kontribusi Fisika Indonesia*. *12*(2), 49–55.

Vozoff, K. (1990). Magnetotellurics: Principles and practice. *Proc. Indian Acad. Sci. (Earth Planet. Sci.)*, *99*(4), 441–471. https://doi.org/10.1258/135626203765947842

Wang, P., Chen, X., & Zhang, Y. (2023). Synthesizing magnetotelluric time series based on forward modeling. *Frontiers in Earth Science*, *11*(February), 1–13. https://doi.org/10.3389/feart.2023.1086749

Wijaya, R. A. K., Bahri, A. S., Warnana, D. D. W., & Darmawan, A. D. (2016). Inversi 1-D Pada Data Magnetotellurik Di Lapangan X Menggunakan Metode Occam Dan Simulated Annealing. *Jurnal Geosaintek*, *2*(2), 75. https://doi.org/10.12962/j25023659.v2i2.1920

Xia, Y., & Ji, Y. (2025). *Application of a novel metaheuristic algorithm inspired by Adam gradient descent in distributed Xia, Y., Ji, Y., 2025. Application of a novel metaheuristic algorithm inspired by Adam gradient descent in distributed permutation flow shop scheduling problem*. 1–61. https://doi.org/https://doi.org/10.1038/s41598-025-01678-9